Low-energy axial-vector transitions from decuplet to octet baryons

Måns Holmberg⬤ and Stefan Leupold

Institutionen för fysik och astronomi, Uppsala Universitet, Box 516, S-75120 Uppsala, Sweden

Axial-vector transitions of decuplet to octet baryons are parametrized at low energies guided by a complete and minimal chiral Lagrangian up to next-to-leading order. It is pointed out that beyond the well-known leading-order term, there is only one contribution at next-to-leading order. This contribution is flavor symmetric. Therefore the corresponding low-energy constant can be determined in any strangeness sector. As functions of this low-energy constant, we calculate the decay widths and Dalitz distributions for the decays of decuplet baryons to octet baryons, pions, and photons and for the weak decay of the Omega baryon to a cascade baryon, an electron, and an antineutrino.

I. INTRODUCTION AND SUMMARY

One of the interesting processes of neutrino-nucleon scattering is the production of the lowest-lying Delta state [1–5]. On the theory side, the relevant quantities are the vector and axial-vector form factors for the transition of a nucleon to a Delta. While the vector transition form factors can also be addressed in the electroproduction of a Delta on a nucleon, information about the axial-vector transition form factors is scarce. Of course, the situation is even worse in the strangeness sector. At least, the decay width of the reaction $\Omega^- \to \Xi^0 e^- \bar{\nu}_e$ has been measured [6,7].

The purpose of the present work is to study the low-energy limit of these axial-vector transition form factors and to point out various ways how to measure these quantities. Recently we have established a complete and minimal relativistic chiral Lagrangian of next-to-leading order (NLO) for the three-flavor sector including the lowest lying baryon octet and decuplet states [8]. Based on this Lagrangian, we will calculate various observables that depend on the low-energy constants (LECs) that enter the axial-vector transition form factors.

Dealing with a chiral baryon Lagrangian at NLO means that we carry out tree-level calculations. But why do we bother about such NLO tree-level results, if the state of the art seems to be one-loop calculations [2,3]? Though axial-vector transition form factors have been calculated at the one-loop level of chiral perturbation theory (χPT), the numerically fairly unknown tree-level contributions have often been formulated based on nonminimal Lagrangians.

In this way, one assumes a too large number of to be fitted parameters, and one misses cross relations between form factors and also between different processes. Therefore we have decided to go one step back and analyze the NLO structure, i.e., tree-level structure of the axial-vector transition form factors. Of course, this can only be the first step of a more detailed investigation that should go beyond the NLO level.

Let us start with the introduction of pertinent axial-vector transition form factors where we can already point out some short-comings of previous works. With B denoting a spin-1/2 baryon from the nucleon octet and B^* a spin-3/2 baryon from the Delta decuplet, the axial-vector transitions can be written as

$$\langle B^*(p')|j_A^\mu|B(p)\rangle = \bar{u}_\nu(p')\Gamma^{\mu\nu}u(p) \tag{1}$$

with $q = p' - p$ and

$$\Gamma^{\mu\nu} = q^\mu q^\nu H_0(q^2) + g^{\mu\nu}H_1(q^2) \\ + (\gamma^\mu q^\nu - \slashed{q}g^{\mu\nu})H_2(q^2) + i\sigma^{\mu\alpha}q_\alpha q^\nu H_3(q^2). \tag{2}$$

The advantage of the decomposition (1), (2) lies in the fact that contributions to the axial-vector transition form factors H_i start only at the ith chiral order for $i = 1, 2, 3$. This is easy to see because the momentum q carried by the axial-vector current is a small quantity of chiral order 1. In particular, this implies that H_3 does not receive contributions from leading order (LO) and from NLO. The "regular" contributions to H_0 start also at third chiral order, but H_0 receives a contribution at LO from a Goldstone-boson pole term.

For the following rewriting, it is of advantage to recall the equations of motion for the spin-1/2 spinors u and the spin-3/2 Rarita-Schwinger vector-spinors [9] u_ν,

$$(\not{p} - m_8)u(p) = 0, \qquad (\not{p}' - m_{10})u_\nu(p') = 0, \quad (3)$$

where $m_{8/10}$ denotes the mass of the considered baryon octet/decuplet state. Note that the mass difference $m_{10} - m_8$ is counted as a small quantity.

The use of the form factor H_3 is not very common. Instead of $i\sigma_{\mu\alpha}q^\alpha q_\nu$ one often uses a structure $p'_\mu q_\nu - p' \cdot q g_{\mu\nu}$; see e.g., [2,3] and references therein. The problem with the latter structure is, however, that it looks like an additional fourth independent term that contributes at NLO. Instead, the decomposition (2) shows that there are only three structures up to and including NLO—and H_0 receives only a Goldstone-boson pole contribution; i.e., there are only two *independent* terms up to and including NLO. The structure $p'_\mu q_\nu - p' \cdot q g_{\mu\nu}$ is *not* required up to and including NLO. To make contact between different ways how to parametrize the transition form factors, one can use a Gordon-type identity,

$$\bar{u}_\nu(-2p'_\mu + (m_{10} + m_8)\gamma_\mu + q_\mu - i\sigma_{\mu\alpha}q^\alpha)u = 0, \quad (4)$$

which can easily be established using the equations of motion (3).

We can now focus on the three form factors H_0, H_1 and H_2, which receive contributions already at LO or NLO, respectively. Using the Lagrangians of LO and NLO from [8] one obtains

$$H_0(q^2) = -\frac{h_A}{\sqrt{2}} \frac{1}{q^2 - m_{\text{GB}}^2} k_f,$$

$$H_1 = \frac{h_A}{\sqrt{2}} k_f,$$

$$H_2 = -2c_E k_f \qquad (5)$$

with the LO low-energy constant h_A and the NLO low-energy constant c_E. The flavor factor k_f depends on the considered channel, i.e., on the flavors of B, B^* and the axial-vector current. Correspondingly, m_{GB} denotes the mass of the Goldstone-boson that can be excited in the considered channel. The flavor factor is extracted from $\epsilon^{ade}\bar{T}^\nu_{abc}(a^\mu)^b_d B^c_e$.

We deduce from (5) the following information: In the NLO approximation, one needs for all the axial-vector decuplet-to-octet transitions only two flavor symmetric low-energy constants. It does not matter in which flavor channels one determines these constants. The main part of this paper is devoted to suggestions how to pin down the NLO low-energy constant c_E.

Obviously, c_E contributes differently than h_A. Thus a minimal and complete NLO Lagrangian must contain a c_E-type structure. It is missing, for instance, in [10]. It might be interesting to explain why this low-energy constant has an index "E" for "electric". At low energies, i.e., in the nonrelativistic limit for the baryons, the dominant contribution for the H_2 form factor stems from γ^0 and from

TABLE I. Determination of h_A from different decay channels of decuplet baryons. We used mixed states in the case of the $\Delta \to N\pi$ decay. The errors come from the experimental uncertainties of the particle masses, decay widths, and branching ratios.

Decay	h_A
$\Delta \to N\pi$	2.87 ± 0.05
$\Sigma^{*+} \to \Lambda\pi^+$	2.39 ± 0.03
$\Sigma^{*+} \to (\Sigma\pi)^+$	2.2 ± 0.1
$\Xi^{*0} \to (\Xi\pi)^0$	2.00 ± 0.06

spatial ν. This selects the combination $q^j a^0 - q^0 a^j$, which constitutes an electric axial-vector field strength.

We close the present section by determining h_A. The corresponding structure of the LO Lagrangian gives rise to decays of decuplet baryons to pions and octet baryons. From each of the measured decay widths, one can extract an estimate for h_A. This is provided in Table I, which is in agreement with [11]. Note that this is an approximation for the decay widths that is accurate up to and including NLO—because there are no additional contributions at NLO [8]. One cannot expect to obtain always the very same numerical result for h_A. But the spread in the obtained values can be regarded as an estimate for the neglected contributions that appear beyond NLO. Indeed, those contributions break the flavor symmetry.

In Sec. II we present the basics of the relevant LO and NLO Lagrangian of baryon octet plus decuplet and Goldstone-boson octet χPT. We also specify the numerical values of the previously determined LECs. This is the first part of the paper. In Sec. III, we specify the relevant interaction terms of the $\Omega^- \to \Xi^0 e^- \bar{\nu}_e$ decay, and we also present the LO and NLO decay width predictions (as a function of c_E). Section IV is outlined similarly to Sec. III but in the case of $B(J = 3/2) \to B(J = 1/2)\gamma\pi$ processes. We close by showing the c_E dependence of the single differential decay width of $\Xi^{*0} \to \Xi^- \pi^+ \gamma$ and finally give some concluding remarks.

II. CHIRAL LAGRANGIAN

The relevant part of the LO chiral Lagrangian for baryons including the spin-3/2 decuplet states is given by [8,12–16]

$$\begin{aligned}
\mathcal{L}^{(1)}_{\text{baryon}} = {}& \text{tr}(\bar{B}(i\not{D} - m_{(8)})B) \\
& + \bar{T}^\mu_{abc}(i\gamma_{\mu\nu\alpha}(D^\alpha T^\nu)^{abc} - \gamma_{\mu\nu}m_{(10)}(T^\nu)^{abc}) \\
& + \frac{D}{2}\text{tr}(\bar{B}\gamma^\mu\gamma_5\{u_\mu, B\}) + \frac{F}{2}\text{tr}(\bar{B}\gamma^\mu\gamma_5[u_\mu, B]) \\
& + \frac{h_A}{2\sqrt{2}}(\epsilon^{ade}\bar{T}^\mu_{abc}(u_\mu)^b_d B^c_e + \epsilon_{ade}\bar{B}^e_c(u^\mu)^d_b T^{abc}_\mu) \\
& - \frac{H_A}{2}\bar{T}^\mu_{abc}\gamma_\nu\gamma_5(u^\nu)^c_d T^{abd}_\mu \quad (6)
\end{aligned}$$

with tr denoting a flavor trace. For mesons the well-known LO chiral Lagrangian is given by [17–19]

$$\mathcal{L}_{\text{meson}}^{(1)} = \frac{F_\pi^2}{4} \text{tr}(u_\mu u^\mu + \chi_+), \tag{7}$$

with $\chi_\pm = u^\dagger \chi u^\dagger \pm u\chi^\dagger u$ and $\chi = 2B_0(s + ip)$ obtained from the scalar and pseudoscalar sources s and p. The low-energy constant B_0 is essentially the ratio of the light-quark condensate and the square of the pion-decay constant; see, e.g., [18–21].

We have introduced the totally antisymmetrized products of two and three gamma matrices [22],

$$\gamma^{\mu\nu} := \frac{1}{2}[\gamma^\mu, \gamma^\nu] = -i\sigma^{\mu\nu} \tag{8}$$

and

$$\gamma^{\mu\nu\alpha} := \frac{1}{6}(\gamma^\mu\gamma^\nu\gamma^\alpha + \gamma^\nu\gamma^\alpha\gamma^\mu + \gamma^\alpha\gamma^\mu\gamma^\nu$$
$$- \gamma^\mu\gamma^\alpha\gamma^\nu - \gamma^\alpha\gamma^\nu\gamma^\mu - \gamma^\nu\gamma^\mu\gamma^\alpha)$$
$$= \frac{1}{2}\{\gamma^{\mu\nu}, \gamma^\alpha\} = +i\epsilon^{\mu\nu\alpha\beta}\gamma_\beta\gamma_5, \tag{9}$$

respectively. Our conventions are $\gamma_5 := i\gamma^0\gamma^1\gamma^2\gamma^3$ and $\epsilon_{0123} = -1$ (the latter in agreement with [22] but opposite to [15,23]). If a formal manipulation program is used to calculate spinor traces and Lorentz contractions a good check for the convention for the Levi-Civita symbol is the last relation in (9).

The spin-$1/2$ octet baryons are collected in (B_b^a is the entry in the ath row, bth column)

$$B = \begin{pmatrix} \frac{1}{\sqrt{2}}\Sigma^0 + \frac{1}{\sqrt{6}}\Lambda & \Sigma^+ & p \\ \Sigma^- & -\frac{1}{\sqrt{2}}\Sigma^0 + \frac{1}{\sqrt{6}}\Lambda & n \\ \Xi^- & \Xi^0 & -\frac{2}{\sqrt{6}}\Lambda \end{pmatrix}. \tag{10}$$

The decuplet is expressed by a totally symmetric flavor tensor T^{abc} with

$$T^{111} = \Delta^{++}, \qquad T^{112} = \frac{1}{\sqrt{3}}\Delta^+,$$

$$T^{122} = \frac{1}{\sqrt{3}}\Delta^0, \qquad T^{222} = \Delta^-,$$

$$T^{113} = \frac{1}{\sqrt{3}}\Sigma^{*+}, \qquad T^{123} = \frac{1}{\sqrt{6}}\Sigma^{*0}, \qquad T^{223} = \frac{1}{\sqrt{3}}\Sigma^{*-},$$

$$T^{133} = \frac{1}{\sqrt{3}}\Xi^{*0}, \qquad T^{233} = \frac{1}{\sqrt{3}}\Xi^{*-}, \qquad T^{333} = \Omega. \tag{11}$$

The Goldstone bosons are encoded in

$$\Phi = \begin{pmatrix} \pi^0 + \frac{1}{\sqrt{3}}\eta & \sqrt{2}\pi^+ & \sqrt{2}K^+ \\ \sqrt{2}\pi^- & -\pi^0 + \frac{1}{\sqrt{3}}\eta & \sqrt{2}K^0 \\ \sqrt{2}K^- & \sqrt{2}\bar{K}^0 & -\frac{2}{\sqrt{3}}\eta \end{pmatrix},$$

$$u^2 := U := \exp(i\Phi/F_\pi), \qquad u_\mu := iu^\dagger(\nabla_\mu U)u^\dagger = u_\mu^\dagger. \tag{12}$$

The fields have the following transformation properties with respect to chiral transformations [12,19]:

$$U \to LUR^\dagger, \qquad u \to Luh^\dagger = huR^\dagger,$$

$$u_\mu \to hu_\mu h^\dagger, \qquad B \to hBh^\dagger,$$

$$T_\mu^{abc} \to h_d^a h_e^b h_f^c T_\mu^{def}, \qquad \bar{T}_{abc}^\mu \to (h^\dagger)_a^d(h^\dagger)_b^e(h^\dagger)_c^f \bar{T}_{def}^\mu. \tag{13}$$

In particular, the choice of upper and lower flavor indices is used to indicate that upper indices transform with h under flavor transformations while the lower components transform with $h^\dagger$.

The chirally covariant derivative for a (baryon) octet is defined by

$$D^\mu B := \partial^\mu B + [\Gamma^\mu, B], \tag{14}$$

for a decuplet T by

$$(D^\mu T)^{abc} := \partial^\mu T^{abc} + (\Gamma^\mu)_{a'}^a T^{a'bc} + (\Gamma^\mu)_{b'}^b T^{ab'c}$$
$$+ (\Gamma^\mu)_{c'}^c T^{abc'}, \tag{15}$$

for an antidecuplet by

$$(D^\mu \bar{T})_{abc} := \partial^\mu \bar{T}_{abc} - (\Gamma^\mu)_a^{a'} \bar{T}_{a'bc} - (\Gamma^\mu)_b^{b'} \bar{T}_{ab'c}$$
$$- (\Gamma^\mu)_c^{c'} \bar{T}_{abc'}, \tag{16}$$

and for the Goldstone boson fields by

$$\nabla_\mu U := \partial_\mu U - i(v_\mu + a_\mu)U + iU(v_\mu - a_\mu) \tag{17}$$

with

$$\Gamma_\mu := \frac{1}{2}(u^\dagger(\partial_\mu - i(v_\mu + a_\mu))u$$
$$+ u(\partial_\mu - i(v_\mu - a_\mu))u^\dagger), \tag{18}$$

where v and a denote external vector and axial-vector sources.

In (7), χ_+ includes the mass term when replacing the scalar source s by the quark mass matrix. As for the baryon masses, $m_{(8)}$ [$m_{(10)}$] in (6) denotes the masses of the octet (decuplet) baryons in the chiral limit. At NLO, octet and decuplet flavor breaking terms appear (containing χ_+) that

are responsible for splitting the baryon masses such that they are sufficiently close to the physical masses [8,24,25]. Therefore, we use the physical masses in practice.

Standard values for the coupling constants are $F_\pi = 92.4$ MeV, $D = 0.80$, $F = 0.46$. For the pion-nucleon coupling constant this implies $g_A = F + D = 1.26$. In the case of H_A, we use estimates from large-N_c considerations: $H_A = \frac{9}{5} g_A \approx 2.27$ [15,23] or $H_A = 9F - 3D \approx 1.74$ [14,26], since we lack a simple direct observable to pin it down. Numerically we use $H_A \approx 2.0$.

At NLO, we have five terms that contribute to the decays of interest [8]: two octet sector terms that are given by

$$b_{M,D}\mathrm{tr}(\bar{B}\{f_+^{\mu\nu}, \sigma_{\mu\nu}B\}) + b_{M,F}\mathrm{tr}(\bar{B}[f_+^{\mu\nu}, \sigma_{\mu\nu}B]), \quad (19)$$

one term from the decuplet sector given by

$$d_M i(\bar{T}_\mu)_{abc}(f_+^{\mu\nu})_d^c T_\nu^{abd}, \quad (20)$$

and finally two decuplet-to-octet transition terms given by

$$ic_M\epsilon_{ade}\bar{B}_c^e\gamma_\mu\gamma_5(f_+^{\mu\nu})_b^d T_\nu^{abc}$$
$$+ ic_E\epsilon_{ade}\bar{B}_c^e\gamma_\mu(f_-^{\mu\nu})_b^d T_\nu^{abc} + \mathrm{H.c.} \quad (21)$$

The field strengths $f_\pm^{\mu\nu}$ are given by

$$f_\pm^{\mu\nu} := uF_L^{\mu\nu}u^\dagger \pm u^\dagger F_R^{\mu\nu}u \quad (22)$$

with

$$F_{R,L}^{\mu\nu} := \partial^\mu(v^\nu \pm a^\nu) - \partial^\nu(v^\mu \pm a^\mu) - i[v^\mu \pm a^\mu, v^\nu \pm a^\nu]. \quad (23)$$

Interactions with external forces are studied by the replacement of the vector and axial-vector sources v^ν, a^ν. For electromagnetic interactions we have the replacement [20],

$$v_\mu \rightarrow eA_\mu \begin{pmatrix} \frac{2}{3} & 0 & 0 \\ 0 & -\frac{1}{3} & 0 \\ 0 & 0 & -\frac{1}{3} \end{pmatrix} \quad (24)$$

with the photon field A_μ and the proton charge e; and for weak interactions mediated by the W-bosons we have the replacement [20],

$$v_\mu - a_\mu \rightarrow -\frac{g_w}{\sqrt{2}}W_\mu^+ \begin{pmatrix} 0 & V_{ud} & V_{us} \\ 0 & 0 & 0 \\ 0 & 0 & 0 \end{pmatrix} + \mathrm{H.c.} \quad (25)$$

with the W-boson field W_μ^+, the Cabibbo-Kobayashi-Maskawa matrix elements V_{ud}, V_{us} [27], and the weak gauge coupling g_w (related to Fermi's constant and the W mass).

The values of the low-energy constants $b_{M,D/F}$ and d_M are determined by fitting the calculated and measured magnetic moments of the octet and decuplet baryons, respectively. The results are: $b_{M,D} \approx 0.321$ GeV^{-1}, $b_{M,F} \approx 0.125$ GeV^{-1}, and $d_M \approx -1.16$ GeV^{-1}. Furthermore, from the radiative decay of a decuplet baryon to an octet baryon and a photon, one obtains $c_M \approx \pm 1.92$ GeV^{-1}. The values of the above NLO LECs come from [8]. Next we present two types of decay channels that can be used to determine c_E and the sign of c_M, starting with $\Omega^- \rightarrow \Xi^0 e^- \bar{\nu}_e$.

In view of the absence of data that one can use to help pin down c_E and the sign of c_M; we stress that the purpose of this paper is to motivate such experiments and not to explore the uncertainties of already determined LECs. Therefore, we stick to the central values of those LECs for numerical results.

III. DECAY PROCESS $\Omega^- \rightarrow \Xi^0 e^- \bar{\nu}_e$

There are two contributing tree-level diagrams at NLO in χPT for the decay of the Omega baryon decaying into a cascade baryon, an electron, and an electron antineutrino. These are shown in Fig. 1.

At LO, we have three contributing terms: the $\sim h_A$ term from (6), the kinetic term for the mesons in (7), as well as the standard weak charged-current interaction term [20]. Going to NLO, we also have the $\sim c_{M/E}$ terms in (21). When calculating the decay width we used *Mathematica* and FeynCalc to perform the traces of the gamma matrices [28,29]. The resulting partial decay width at NLO contains terms proportional to h_A^2, c_E^2, c_M^2 and $h_A c_E$. Figure 2 illustrates the calculated and measured branching ratio. We use the values of the LECs described in Sec. II together with $h_A = 2.0$, i.e., the value of h_A obtained from fitting the partial decay width of $\Xi^* \rightarrow \Xi\pi$ to data, again see Table I.

We then fit the NLO branching ratio to the measurement, resulting in c_E: (0.5 ± 1) GeV^{-1} and (-5 ± 1) GeV^{-1}. The error comes from the experimental uncertainty of the branching ratio. We cannot distinguish between the two solutions of c_E by only considering the integrated decay width, and likewise, we cannot pin down the sign of c_M since the partial decay width contains no linear c_M term.
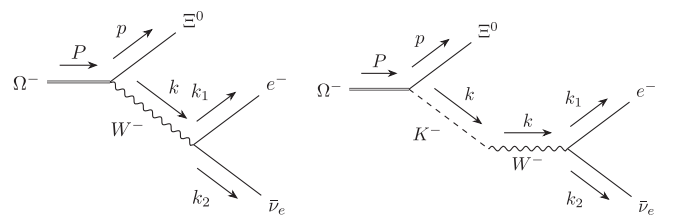

FIG. 1. Diagrams contributing to the decay of $\Omega^- \rightarrow \Xi^0 e^- \bar{\nu}_e$. These two diagrams are the only two topologically distinct diagrams at NLO, but note that the $\Omega\Xi W$-vertex comes from three terms.
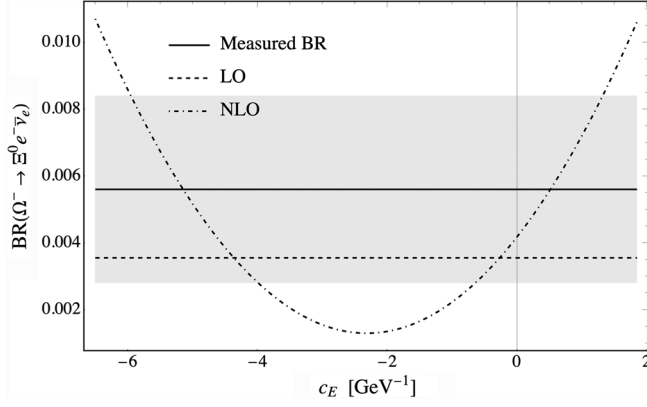
FIG. 2.   NLO branching ratio of $\Omega^- \to \Xi^0 e^- \bar{\nu}_e$ as a function of c_E, together with the LO result and the experimental value [7]. The gray box illustrates the measurement uncertainty.

We can instead study the distribution of the double differential decay width to obtain more information. In Fig. 3 we illustrate the double differential decay distribution for the four different solutions of c_M and c_E in the frame where the electron and antineutrino goes back to back, i.e., $\vec{k}_1 + \vec{k}_2 = 0$. We chose to work with the kinematic variables $m^2(e^-\bar{\nu}_e)$ and $\cos(\theta)$, where θ is the angle between the three-momenta of the cascade baryon and the electron. With enough statistics, it would be possible to distinguish between all four cases, and even with less statistics, it could be possible to at least determine the relative sign of c_M and c_E, depending on where one
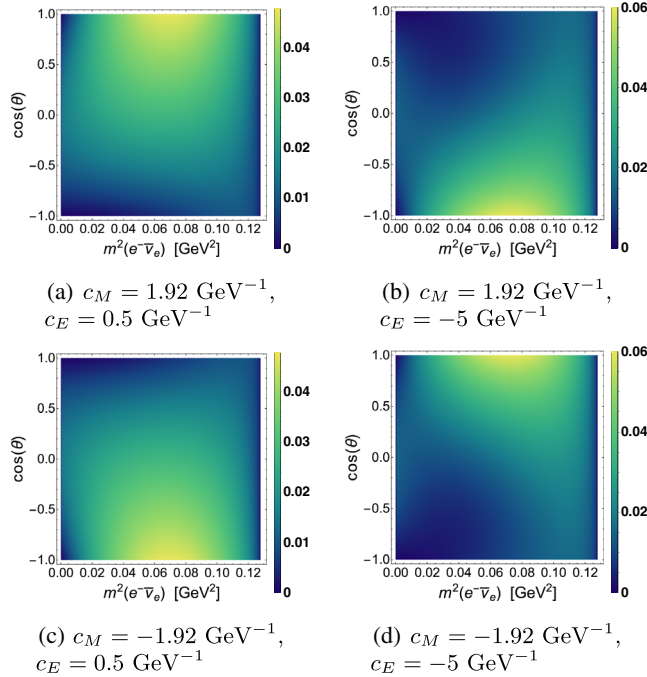
finds the majority of events in the Dalitz plots [i.e., closer to $\cos(\theta) = 1$ or $\cos(\theta) = -1$]. Note also that there is an apparent antisymmetry such that $c_M \to -c_M$ is equivalent to $\cos(\theta) \to -\cos(\theta)$. This is, however, only approximately true when the lepton masses are small compared to the hadron masses. In the case of vanishing lepton masses, we find that all linear terms of $\cos(\theta)$ in the double differential decay width are proportional to c_M. This phenomenon is called forward-backward asymmetry [30].

IV. DECAY PROCESSES
$B(J=3/2) \to B(J=1/2)\gamma\pi$

For the decay of a decuplet baryon into an octet baryon, a pion and a photon we have six diagrams at NLO in χPT. These diagrams are shown in Fig. 4. The interaction terms are given by all terms in (6), (7), (19), (20), and (21).

As before, we use Mathematica and FeynCalc to perform the traces of the gamma matrices. Furthermore, we explicitly checked that the Ward identity for the electromagnetic current holds, that is $\mathcal{M}_\mu k^\mu = 0$ for all decays.

Concerning the values of the different LECs, we used $h_A = 2.4$, being the average value of Table I, together with $c_M = +1.92 \text{ GeV}^{-1}$ and $c_E = 0.5 \text{ GeV}^{-1}$. The decays contain infrared divergences resulting from final-state radiation that, in the limit of vanishing photon energy, can make a propagating particle on shell [22]. Therefore, we used a cutoff of the photon energy at 25 MeV (in the

(a) $c_M = 1.92 \text{ GeV}^{-1}$, $c_E = 0.5 \text{ GeV}^{-1}$

(b) $c_M = 1.92 \text{ GeV}^{-1}$, $c_E = -5 \text{ GeV}^{-1}$

(c) $c_M = -1.92 \text{ GeV}^{-1}$, $c_E = 0.5 \text{ GeV}^{-1}$

(d) $c_M = -1.92 \text{ GeV}^{-1}$, $c_E = -5 \text{ GeV}^{-1}$

FIG. 3.   The double differential decay distribution of $\Omega^- \to \Xi^0 \bar{\nu}_e e^-$ for the two solutions of c_E and for different signs of c_M. The scale of the double differential decay distribution is linear with an arbitrary normalization.
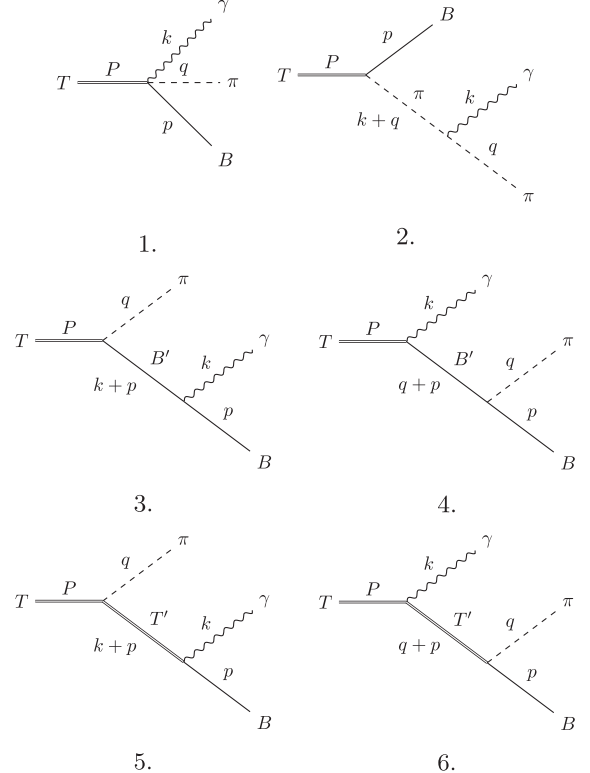

FIG. 4.   Diagrams contributing to the decay of a decuplet baryon into an octet baryon, a pion and a photon.

TABLE II.   Branching ratios at LO and NLO of all energetically possible $B^*(J = 3/2) \to B\pi\gamma$ decays allowed by flavor symmetry, except $\Sigma^{*\pm} \to \Lambda\pi^{\pm}\gamma$ that run over the pole of Σ^0. The second column is showing the LEC dependence at NLO.

Decay	LEC dependence at NLO	BR at LO	BR at NLO
$\Xi^{*-} \to \Xi^-\pi^0\gamma$	$h_A, d_M, b_{M,D}, b_{M,F}$	8.2×10^{-6}	8.6×10^{-6}
$\Xi^{*-} \to \Xi^0\pi^-\gamma$	$h_A, H_A, c_M, c_E, d_M, b_{M,D}$	1.4×10^{-3}	1.4×10^{-3}
$\Xi^{*0} \to \Xi^-\pi^+\gamma$	$h_A, D, F, c_M, c_E, b_{M,D}, b_{M,F}$	1.2×10^{-3}	1.2×10^{-3}
$\Xi^{*0} \to \Xi^0\pi^0\gamma$	$h_A, H_A, D, F, c_M, b_{M,D}$	0	1.9×10^{-6}
$\Sigma^{*+} \to \Sigma^+\pi^0\gamma$	$h_A, H_A, D, c_M, d_M, b_{M,D}, b_{M,F}$	8.9×10^{-7}	1.2×10^{-6}
$\Sigma^{*+} \to \Sigma^0\pi^+\gamma$	$h_A, H_A, F, c_M, c_E, d_M, b_{M,D}$	3.6×10^{-5}	3.7×10^{-5}
$\Sigma^{*-} \to \Sigma^-\pi^0\gamma$	$h_A, d_M, b_{M,D}, b_{M,F}$	6.3×10^{-7}	6.6×10^{-7}
$\Sigma^{*-} \to \Sigma^0\pi^-\gamma$	$h_A, H_A, c_M, c_E, d_M, b_{M,D}$	4.4×10^{-5}	4.5×10^{-5}
$\Sigma^{*0} \to \Sigma^+\pi^-\gamma$	$h_A, H_A, D, F, c_M, c_E, b_{M,D}, b_{M,F}$	5.9×10^{-5}	5.9×10^{-5}
$\Sigma^{*0} \to \Sigma^-\pi^+\gamma$	$h_A, D, F, c_M, c_E, b_{M,D}, b_{M,F}$	3.3×10^{-5}	3.4×10^{-5}
$\Sigma^{*0} \to \Sigma^0\pi^0\gamma$	$h_A, D, c_M, b_{M,D}$	0	2.6×10^{-8}
$\Sigma^{*0} \to \Lambda\pi^0\gamma$	$h_A, D, c_M, b_{M,D}$	0	3.6×10^{-6}
$\Delta^{++} \to p\pi^+\gamma$	$h_A, H_A, c_M, c_E, d_M, b_{M,D}, b_{M,F}$	1.7×10^{-3}	1.8×10^{-3}
$\Delta^+ \to p\pi^0\gamma$	$h_A, H_A, D, F, c_M, d_M, b_{M,D}, b_{M,F}$	5.6×10^{-5}	7.2×10^{-5}
$\Delta^+ \to n\pi^+\gamma$	$h_A, H_A, D, F, c_M, c_E, d_M, b_{M,D}$	7.5×10^{-4}	7.6×10^{-4}
$\Delta^0 \to p\pi^-\gamma$	$h_A, H_A, D, F, c_M, d_M, b_{M,D}, b_{M,F}$	1.0×10^{-3}	1.0×10^{-3}
$\Delta^0 \to n\pi^0\gamma$	$h_A, H_A, D, F, c_M, b_{M,D}$	0	7.6×10^{-6}
$\Delta^- \to n\pi^-\gamma$	$h_A, H_A, c_M, c_E, d_M, b_{M,D}$	2.3×10^{-3}	2.3×10^{-3}

frame where $\vec{p} + \vec{q} = 0$), roughly corresponding to the lowest detectable photon energy at the upcoming $\overline{\text{P}}$ANDA experiment (Antiproton ANnihilation in DArmstadt) [31–33] and the Beijing Spectrometer III [34]. This cutoff can be arbitrarily chosen to match the photon energy resolution of any experiment. In Table II, we have collected the predictions of all energetically possible decays and their branching ratios at LO and NLO as well as the LEC dependence.

Looking at Table II we see that decay widths containing only neutral states vanish at LO, which is only natural since neutral hadrons do not interact with photons at LO. Contributions with LO LECs appear at NLO since the amplitudes contain structures which are proportional to products of LO and NLO LECs, e.g., diagram 3 gives terms like $\sim h_A b_{M,D}$, but with absent pure LO contributions. Furthermore, it is reassuring that the branching ratios of these neutral decays are small at NLO since they vanish at LO; indicating that the NLO contribution is, in general, a small correction.

The branching ratios of decays with neutral pions in the final state are small due to the same reason, that is, since the pion-pion-photon vertex forbids neutral pions, the otherwise large contribution of the pion propagator in diagram 2 disappear.

Let us briefly investigate the possible ranges of the different LECs due to their uncertainty, starting with H_A. Varying the value of H_A by ± 0.3 changes the decay widths insignificantly (much less than 1%), except in the cases of $\Xi^{*0} \to \Xi^0\pi^0\gamma$ and $\Delta^0 \to n\pi^0\gamma$ which change by 10% and 2%, respectively. We also considered $c_M = -1.92 \text{ GeV}^{-1}$, which changes the decay widths by a few percents (often

much less) in the case of decays involving charged states. The four decays with only neutral states (and vanishing decay width at LO) changed significantly (up to 80%). But since they vanish at LO they are prone to be more sensitive to the values of the NLO LECs.

Once data are available, we can use these radiative three-body decays to further investigate c_E. For this purpose, the decays $\Xi^{*-} \to \Xi^0\pi^-\gamma$ and $\Xi^{*0} \to \Xi^-\pi^+\gamma$ are of most interest, since they both have a relatively large branching ratio of $\sim 10^{-3}$ and because of the small (total) decay width of cascade baryons (as compared to broad
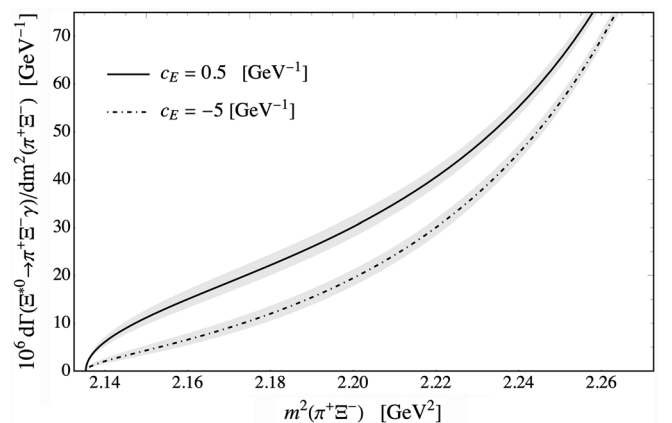

FIG. 5.   Impact of the two solutions of c_E on the single differential decay width of $\Xi^{*0} \to \Xi^-\pi^+\gamma$ using $c_M = +1.92 \text{ GeV}^{-1}$. We plot the single differential decay width down to a photon energy of 50 MeV (otherwise the c_E-dependence is hard to display). The gray intervals come from the uncertainty of the two solutions of c_E.

Delta baryons). We find that the decay widths of these two cascade decays decrease by around 20% when changing to the negative c_E solution. In Fig. 5 we consider how the single differential decay width of $\Xi^{*0} \to \Xi^- \pi^+ \gamma$ changes when varying c_E.

We note that at low photon energies both solutions of c_E converge, in the region where the single differential decay width blows up, due to the infrared divergence. Instead, it is at higher photon energies, i.e., lower $m^2(\pi^+ \Xi^-) = M_\Xi^2 - 2M_\Xi E_\gamma$, where we can distinguish between the two possible c_E.

To conclude, we provide two types of decay channels that can be used to probe the axial-vector transition of a decuplet to an octet baryon, parametrized by c_E. The most promising decays for this purpose are $\Omega^- \to \Xi^0 e^- \bar{\nu}_e$, $\Xi^{*-} \to \Xi^0 \pi^- \gamma$, and $\Xi^{*0} \to \Xi^- \pi^+ \gamma$. Moreover, by studying the double differentiable decay distribution of the Omega decay, one can determine the sign of c_M. We hope that such experiments can be carried out at $\bar{P}ANDA$ and in part at BES III.

ACKNOWLEDGMENTS

[1] L. Alvarez-Ruso *et al.*, Prog. Part. Nucl. Phys. **100**, 1 (2018).

[2] M. Procura, Phys. Rev. D **78**, 094021 (2008).

[3] L. S. Geng, J. Martin Camalich, L. Alvarez-Ruso, and M. J. Vicente Vacas, Phys. Rev. D **78**, 014011 (2008).

[4] U. Mosel, Phys. Rev. C **91**, 065501 (2015).

[5] Y. Ünal, A. Küçükarslan, and S. Scherer, Phys. Rev. D **99**, 014012 (2019).

[6] M. Bourquin *et al.* (Bristol-Geneva-Heidelberg-Orsay-Rutherford-Strasbourg Collaboration), Nucl. Phys. **B241**, 1 (1984).

[7] M. Tanabashi *et al.* (Particle Data Group Collaboration), Phys. Rev. D **98**, 030001 (2018).

[8] M. Holmberg and S. Leupold, Eur. Phys. J. A **54**, 103 (2018).

[9] W. Rarita and J. Schwinger, Phys. Rev. **60**, 61 (1941).

[10] S.-Z. Jiang, Y.-R. Liu, H.-Q. Wang, and Q.-H. Yang, Phys. Rev. D **97**, 054031 (2018).

[11] C. Granados, S. Leupold, and E. Perotti, Eur. Phys. J. A **53**, 117 (2017).

[12] E. E. Jenkins and A. V. Manohar, Phys. Lett. B **259**, 353 (1991).

[13] M. F. M. Lutz and E. E. Kolomeitsev, Nucl. Phys. **A700**, 193 (2002).

[14] A. Semke and M. F. M. Lutz, Nucl. Phys. **A778**, 153 (2006).

[15] V. Pascalutsa, M. Vanderhaeghen, and S. N. Yang, Phys. Rep. **437**, 125 (2007).

[16] T. Ledwig, J. Martin Camalich, L. S. Geng, and M. J. Vicente Vacas, Phys. Rev. D **90**, 054502 (2014).

[17] S. Weinberg, Physica (Amsterdam) **96A**, 327 (1979).

[18] J. Gasser and H. Leutwyler, Nucl. Phys. **B250**, 465 (1985).

[19] S. Scherer and M. R. Schindler, *A Primer for Chiral Perturbation Theory*, Lecture Notes in Physics Vol. 830 (Springer, Berlin, Heidelberg, 2012).

[20] S. Scherer, in *Advances in Nuclear Physics* edited by J. W. Negele and E. W. Vogt (Springer, Boston, MA, 2003), Vol. 27, pp. 277–538.

[21] J. Gasser and H. Leutwyler, Ann. Phys. (N.Y.) **158**, 142 (1984).

[22] M. E. Peskin and D. V. Schroeder, *An Introduction to Quantum Field Theory* (Westview Press, Boca Raton, Florida, 1995).

[23] T. Ledwig, J. Martin-Camalich, V. Pascalutsa, and M. Vanderhaeghen, Phys. Rev. D **85**, 034013 (2012).

[24] J. A. Oller, M. Verbeni, and J. Prades, J. High Energy Phys. 09 (2006) 079.

[25] M. Frink and U.-G. Meißner, Eur. Phys. J. A **29**, 255 (2006).

[26] R. F. Dashen and A. V. Manohar, Phys. Lett. B **315**, 425 (1993).

[27] M. Kobayashi and T. Maskawa, Prog. Theor. Phys. **49**, 652 (1973).

[28] Wolfram Research, Inc., *Mathematica* (Champaign, IL, 2019), https://support.wolfram.com/kb/472.

[29] R. Mertig, M. Böhm, and A. Denner, Comput. Phys. Commun. **64**, 345 (1991).

[30] J. Donoghue, E. Golowich, and B. Holstein, *Dynamics of the Standard Model*, Cambridge Monographs on Particle Physics, Nuclear Physics and Cosmology (Cambridge University Press, Cambridge, England, 1994).

[31] E. Thomé, Multi-strange and charmed antihyperon-hyperon physics for $\bar{P}ANDA$, Ph.D. thesis, Uppsala U, 2012.

[32] M. F. M. Lutz *et al.* (PANDA Collaboration), arXiv: 0903.3905.

[33] W. Erni *et al.* (PANDA Collaboration), arXiv:0810.1216.

[34] M. Ablikim *et al.* (BESIII Collaboration), Nucl. Instrum. Methods Phys. Res., Sect. A **614**, 345 (2010).